Available online at www.sciencedirect.com
ScienceDirect
Journal of Non-Crystalline Solids 354 (2008) 2472–2477
JOURNAL OF NON-CRYSTALLINE SOLIDS
www.elsevier.com/locate/jnoncrysol

Efficient ITO–Si solar cells and power modules fabricated with a low temperature technology: Results and perspectives

O. Malik *, F.J. De la Hidalga-W, C. Zúñiga-I, G. Ruiz-T

Electronics Department, National Institute for Astrophysics, Optics and Electronics, INAOE, P.O. Box 51 & 216, Puebla 72000, Mexico

Available online 20 February 2008

Abstract

ITO–SiO_x–*n*Si semiconductor–insulator–semiconductor (SIS) structures have been produced with a simple spraying technique. It is shown that the structures obtained in such a way may be considered as an induced p–n diode, in which the polycrystalline tin–doped indium oxide (ITO) layer spray deposited on the preliminary treated silicon surface leads to an inversion p-layer at the interface. Solar cells with an active area of 1–4 cm^2 have been fabricated based on ITO–SiO_x–*n*Si structures and studied. Under AM0 illumination conditions, the efficiency is nearly 11%, whereas it exceeds 12% for AM1.5 illumination conditions. The theoretical analysis provided in this work shows a good agreement with experimental results and allows for predicting the efficiency of the cells depending on the silicon electro-physical properties.

PACS: 84.60.Jt; 73.40.−c; 85.30.De

Keywords: Silicon; Solar cells; Photovoltaics; Indium tin oxide and other transparent conductors

1. Introduction

For several years a new class of photovoltaic devices, namely the semiconductor–insulator–semiconductor (SIS) solar cells, has emerged [1–5]. The top layer of these diodes is fabricated with a compound indium–tin oxide (ITO). The ITO film can also operate as a metal in structures metal–insulator–semiconductor (MIS), since this is a transparent wide bandgap semiconductor. From the fabrication point of view, such SIS structure is probably the simplest one, because a minimum of fabrication steps are required, and it is compatible with any semiconductor. This is particularly important when polycrystalline semiconductors are used, since it avoids the problem of diffusion of impurities along the grain boundaries during the fabrication. These features make SIS solar cells very promising for large scale terrestrial applications.

The basic purpose of this article is to present results obtained experimentally for ITO–SiO_x–*n*Si solar cells, to compare the properties of these cells with other published results, and to discuss the possible features of these structures based on the provided theoretical analysis.

2. Fabrication, measurements, and modeling of the solar cells

The spray pyrolysis technique was employed for the deposition of the thin ITO films on the surface of a 10 Ω cm n-type silicon substrate that previously was chemically treated. The precursor alcoholic solution contains metallic salts of indium and tin in the form of $InCl_3$ and $SnCl_4$, respectively. Various doping concentrations of tin were obtained by varying the atomic percentage of $SnCl_4$ in the precursor solution. The Sn/In ratio in the solution near 5 at.%, and a substrate temperature of 480 °C were found to be the optimal for obtaining a film with the minimal surface resistance and maximal transparency (∼85%) in the ultraviolet-near infrared spectral range. The metallic

* Corresponding author. Tel./fax: +52 222 247 0517.
E-mail address: amalik@inaoep.mx (O. Malik).

0022-3093/$ - see front matter © 2007 Elsevier B.V. All rights reserved.
doi:10.1016/j.jnoncrysol.2007.09.028

salt solution decomposes pyrolitically to oxide films when sprayed onto the hot substrate.

The 80 nm thick films with a sheet resistance of 30 Ω/□ were deposited on both type of substrates, silicon to form solar cells and sapphire to control the transparency of the films. Additional details regarding the deposition of the films can be found in [6]. The structure of the spray deposited ITO film is polycrystalline with a columnar orientation of grains in the (1 0 0) direction. The ITO films have the properties of a wide-gap (an optical energy gap $E_g^{opt} = 3.7$ eV) degenerated n-type semiconductor with a carrier concentration of about 10^{21} cm^{-3}, and thus with the Fermi level (E_f) lying inside the conduction band (E_c) giving place to the Burstein–Moss effect ($\Delta E^{BM} \approx 0.6$ eV).

Before the deposition of the ITO film, the silicon wafer was cleaned by an HF dip. Deposition of the ITO film on the cleaned silicon surface leads to the formation of a Schottky contact with a high value of the dark current that limits the cell efficiency. In order to increase the efficiency, the surface potential needs to be increased too. This is possible if at the n-type silicon surface an insulator layer with a negative charge exist. Of course, this insulator needs to be very thin to allow the exchange of carriers between the silicon and the indium oxide film. For this purpose, an ultra thin (∼15–17 Å thick) SiO_x layer was grown on the Si surface by immersing the wafer in a hot hydrogen peroxide solution during 10 min. Due to the joint action of the HO_2^- negative charged ions incorporated in the SiO_x film [7] and a significant difference in work functions between the spray deposited ITO film and the silicon substrate, a potential barrier $\phi_b \approx 0.9$ V occurs at Si–SiO_x interface; this was determined experimentally from I–V and C–V measurements. The question is what physical model describes such structure with a so high potential barrier? Two models could be possible: a Schottky barrier structure and an inversion p–n junction. These models are very different from the point of view of the minority carrier concentration $p_s(x = 0)$ near the silicon surface. The first model requires that $p_s(x = 0) \ll N_d$, where N_d is the donor concentration in the silicon substrate. In contrast, the second model is valid for either $p_s \geqslant N_d$ or in strong inversion conditions of the silicon surface. For this case, the energy-band diagram of the structure in equilibrium is that shown in Fig. 1. The condition of strong inversion [8] requires that

$$q\varphi_s \geqslant 2(E_F - E_i), \tag{1}$$

with

$$E_F - E_i = kT \ln(N_d/n_i), \tag{2}$$

and φ_s is the surface potential at the Si/SiO_x interface, q is elementary charge, k is the Boltzmann constant, T is the temperature, n_i is the intrinsic carrier concentration and N_d is the donor concentration in the silicon substrate.

On the other hand,

$$q\varphi_s = q\varphi_b - (E_C - E_F), \tag{3}$$

$$E_C - E_F = kT \ln(N_C/N_d), \tag{4}$$

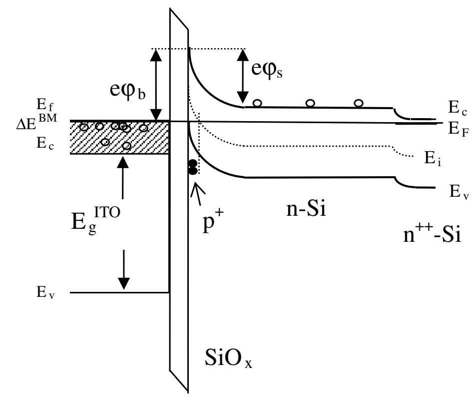

Fig. 1. Energy-band diagram of the ITO–SiO_x–nSi surface-barrier structure in equilibrium.

where N_C is the effective density of states in the conduction band.

Combining Eqs. (1)–(4), it is possible to obtain the condition for the barrier height at the Si/SiO_x interface for a strong inversion of the conductivity type

$$\varphi_b \geqslant kT/q \ln(N_d N_C/n_i^2). \tag{5}$$

For Schottky barrier structures, φ_b needs to be significantly lower than $kT/q \ln(N_d N_C/n_i^2)$. This situation is shown in Fig. 2, where the two possible models are shown in coordinates of a resistivity of the substrate vs. the barrier height. The two shaded areas are related to the two possible models using the well known theory. For instance, if the barrier height is 0.7 V, a horizontal line with this barrier height takes two intercepts: one with the border of the area that is related to a Schottky barrier model, and the other one with the border of the area that is valid for the p–n inversion model. One can see, for a substrate resistivity from 10^{-1} to 10 Ω cm, the structure with this value of the barrier operates as a Schottky barrier. However, above 10^4 Ω cm it could be considered as a n inversion p$^+$–n structure. With the potential height of 0.9 V achieved in this work (for 10 Ω cm silicon substrates treated with the hydrogen perox-

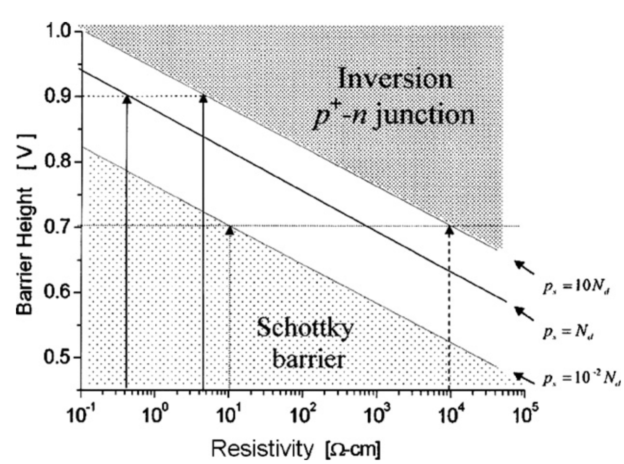

Fig. 2. Two possible models shown in coordinates of the resistivity of the substrate vs. the barrier height.

ide solution by 10 min), the structures may be considered uniquely as a symmetrical p–n ($p_s = N_d$) or as an asymmetrical p$^+$–n junctions ($p_s \geqslant 10N_d$) for a range of substrate resistivity from 0.3 to 10^4 Ω cm. We will use this fact for the theoretical analysis of our structure.

When the intermediate SiO_x layer is sufficiently 'transparent' for the carriers, the tunneling current through this layer provides an Ohmic contact between the ITO film and the surface-induced p$^+$-Si layer.

A Cr/Ni film was deposited at the bottom of the silicon substrate, where previously an n^{++} layer was fabricated by diffusion of phosphorus from an organic film deposited using the spin-off technique. A Cr/Cu/Ni film, in the form of grid, was deposited on the ITO surface as a collector contact. After the fabrication, the parameters of the solar cells with an area of 1–4 cm^2 were measured under AM0 (136 mW/cm^2) illumination.

3. Experimental results

In an earlier report [9] we showed experimental evidences that ITO–SiO_x–*n*Si structures, fabricated on silicon substrates with a resistivity above 1 Ω cm and presenting a 0.8–0.9 eV potential barrier at the silicon interface, should be considered as a minority carrier device (like p/n junctions), with diffusion limited dark current when the oxide layer is sufficiently thin that tunneling does not limit the dark current. The validity of our conclusions is in agreement with other published works [10,11], in which SIS (or MIS) solar cells with an inversion layer have been investigated.

Fig. 3 shows the experimentally obtained dependence of the short-circuit current density (J_{sc}) on the open-circuit voltage (V_{oc}) for the solar cell with an area of 1 cm^2, which was fabricated by the technique described above. The J_{sc}–V_{oc} dependence gives us similar information to that from the dark *J*–*V* characteristics, but allows for eliminating the influence of the serial resistance at a higher current. The light intensity was the variable parameter for such measurement, and each value of J_{sc} and V_{oc} was obtained at some fixed light intensity. An inspection of the characteristics shows that two operating regions can be identified: one at a low voltage with slope $\gamma > 2$, and one at a higher voltage with slope $\gamma \approx 1$. The characteristics at low voltage can be explained due to carriers' recombination in defect centers in the depletion region as well as due to a leakage through surface channels. The influence of the depletion region recombination current on the conversion efficiency of a Si p–n junction working under normal illumination (AM0 or AM1.5) is usually negligible. The same applies to other defect currents. For solar cell applications, the second region of the *I*–*V* characteristics at higher voltage corresponding to the diffusion current is important. The extrapolation of this part of the *I*–*V* characteristic to zero voltage (~10^{-11} A/cm^2 for Fig. 3) gives the saturation dark current density and determines the open-circuit voltage of the solar cell.

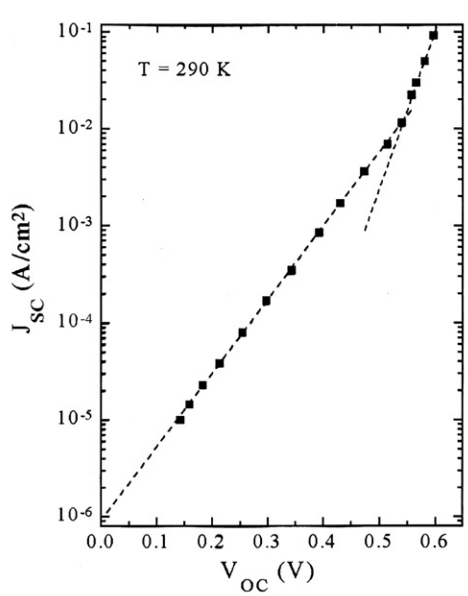

Fig. 3. Dependence of the short-circuit current density (J_{sc}) on the open-circuit voltage (V_{oc}).

Fig. 4 presents the *I*–*V* characteristics of the solar cells obtained under AM0 illumination. The solar cells were fabricated with different treatment times in a hot solution of H_2O_2. One can see that the duration of this treatment influences drastically the *I*–*V* characteristics under illumination. Without treatment, the solar cell is based on the Schottky barrier structure, in which the band-bending at the silicon surface is not enough for obtaining a carrier inversion of the silicon substrate. For 10 min of treatment in H_2O_2, the band-bending at the silicon interface is so high that an inversion p$^+$-layer is formed and the structure now operates as a standard p$^+$–*n* junction. Subsequent continuation of the treatment in a hot hydrogen peroxide solution leads to a decreasing conversion efficiency of the solar cells, this is due to the formation of a thicker SiO_x layer that introduces an additional series resistance and reduces sufficiently the fill factor of the solar cell.

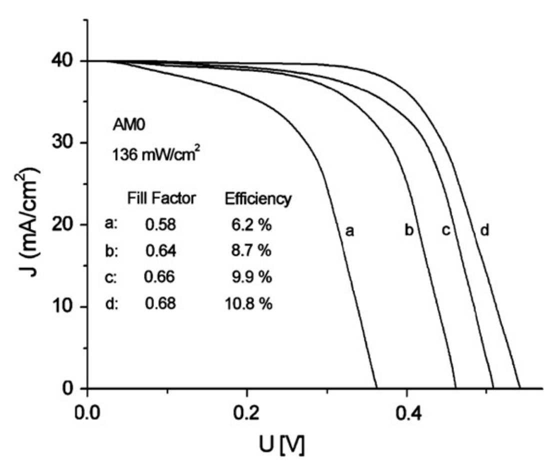

Fig. 4. *I*–*V* curves obtained experimentally for the ITO–SiO_2–*n*Si cells under illumination and for different treatment times in the hot H_2O_2 (minutes): a, 0; b, 2.5; c, 5; d, 10.

We also used a tungsten lamp with a water filter as the light source in order to measure the characteristics of the solar cells in conditions similar to the atmospheric mass 2 (AM2, 75 mW/cm^2). A small fan prevented the cell from heating.

The best conversion efficiency obtained for the solar cells with 10 min treatment in the hydrogen peroxide solution is 12.2%. Due to the vicinity of this spectral distribution to the irradiation from the Sun at atmospheric mass 2 and 1.5, one can expect nearly the same efficiency of the ITO–SiO_x–nSi solar cells under AM1.5 illumination conditions. Results obtained experimentally are compared with theoretical calculations in the next part of the article.

4. Theoretical efficiency of ITO–SiO_x–nSi solar cells

Besides comparing the experimental with theoretical results, in this part of the manuscript we predict the ITO–SiO_x–nSi solar cells properties as a function of the silicon substrate parameters (resistivity and diffusion length of minority carriers). For all the calculations, the thickness of the silicon substrate, thickness and sheet resistance of the ITO film were taken as $d = 500\ \mu$m, $t = 80$ nm and 30 Ω/□, respectively. We considered the case when the diffusion length of minority carriers is shorter than the thickness of the silicon substrate and assumed that the carrier recombination rate on the back contact of the silicon substrate is infinite.

In order to calculate the theoretical parameters of the solar cells we assumed also that the equation for the J–V characteristic of these cells is [8]

$$\ln\left(\frac{J + J_{sc}}{J_0} - \frac{V - JR_s}{J_0 R_{sh}} + 1\right) = \frac{q}{\gamma kT}(V - JR_s), \tag{6}$$

where J is the current density, J_0 the saturation dark current density, J_{sc} is the short-circuit current density, V is output voltage of the solar cell, R_s and R_{sh} are the series and shunt resistances ($\Omega\,cm^2$) of the solar cell, and γ is the 'ideality' factor of the cell. In our calculations, $\gamma = 1$ according to the experimental results shown in Fig. 3.

The calculation of the integral density for the photocurrent, based on the spectral distribution of the incident solar radiation, and the parameters of silicon (absorption coefficient $\alpha(\lambda)$, diffusion length of minority carriers L_p, and thickness of the silicon substrate d) is based on the next equation [12]

$$J_{sc} = q\int_{\lambda 1}^{\lambda 2}\left\{(1-R)_\lambda F_\lambda\left(\frac{\alpha L_p}{\alpha^2 L_p^2 - 1}e^{-\alpha W}\right)\times\left(\alpha L_p - \frac{\cosh\left(\frac{d}{L_p}\right) - e^{-\alpha d}}{\sinh\left(\frac{d}{L_p}\right)}\right)i + \left(1-R\right)_\lambda F_\lambda(1 - e^{-\alpha W})\right\}d\lambda, \tag{7}$$

where q is the electron charge, W is the depletion width in the silicon substrate and $R(\lambda)$ is the spectral reflectance from the ITO/Si interface [13]

$$R(\lambda) = \frac{(g_1^2 + h_1^2)e^{2\alpha_1} + (g_2^2 + h_2^2)e^{-2\alpha_1} + A\cos(2\gamma_1) + B\sin(2\gamma_1)}{e^{2\alpha_1} + (g_1^2 + h_1^2)(g_2^2 + h_2^2)e^{-2\alpha_1} + C\cos(2\gamma_1) + D\sin(2\gamma_1)}, \tag{8}$$

$$g_1 = \frac{1 - n^2 - k^2}{(1+n)^2 + k^2} \quad g_2 = \frac{n^2 - n_1^2 + k^2 - k_1^2}{(n+n_1)^2 + (k+k_1)^2},$$
$$h_1 = \frac{2k}{(1+n)^2 + k^2} \quad h_2 = \frac{2(nk_1 - n_1 k)}{(n+n_1)^2 + (k+k_1)^2},$$
$$\alpha_1 = \frac{2\pi kt}{\lambda} \quad \gamma_1 = \frac{2\pi nt}{\lambda},$$
$$A = 2(g_1 g_2 + h_1 h_2) \quad B = (g_1 h_2 - g_2 h_1),$$
$$C = 2(g_1 g_2 - h_1 h_2) \quad D = (g_1 h_2 + g_2 h_1),$$

where n, n_1 and k, k_1 are the refractive index and the extinction coefficient of the ITO film and Si at a given wavelength λ, respectively, t is the thickness of the ITO film.

The spectral distribution F_λ of the solar radiation related the AM0 (136 mW/cm^2) and AM1.5 (100 mW/cm^2) conditions have been used in the calculations according to the 2000 ASTME-490-00 and ASTM G-173-03 standards, respectively. The optical constants of the ITO film and Si were used from Filmetrics Inc. [14].

The calculated spectral reflectance $R(\lambda)$ of the ITO/Si and the responsivity $S(\lambda)$ of the solar cells as a function of the diffusion length L_p are shown in Fig. 5. The higher photo response in the near infra-red spectral region is a consequence of a higher value of L_p.

One can also see the perfect anti-reflecting properties of the conducting ITO film deposited on the silicon surface.

Fig. 6 shows the dependence of the short-circuit current density J_{sc} calculated according to Eq. (7) under AM0 and AM1.5 conditions.

The values of the open-circuit voltage under AM0 and AM1 conditions were calculated according to the equation

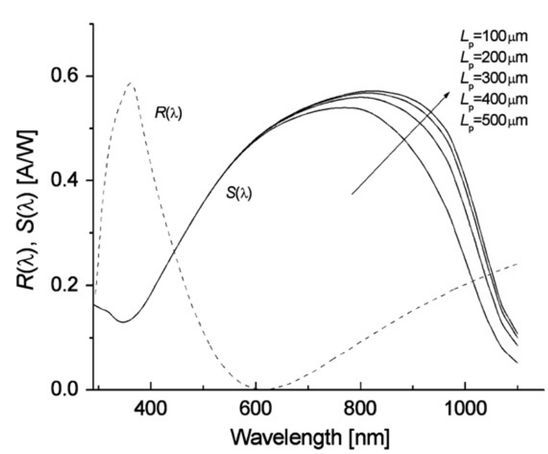

Fig. 5. Spectral reflectance $R(\lambda)$ from the ITO/Si solar cell and responsivity $S(\lambda)$ of the cells as a function of calculated the diffusion length L_p.

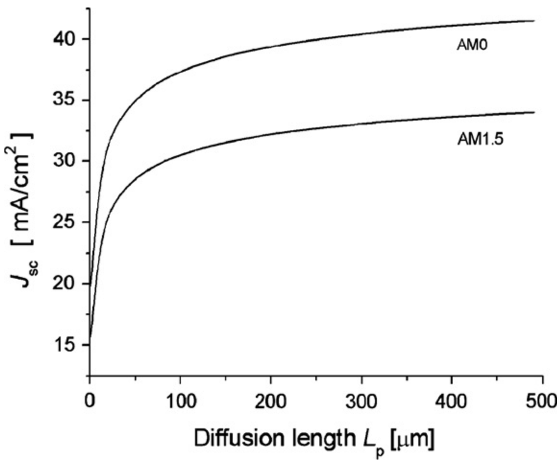

Fig. 6. Dependence of the short-circuit current density J_{sc} calculated according to Eq. (7) under both AM0 and AM1.5 conditions.

$$V_{oc} = \frac{\gamma kT}{q} \ln\left(\frac{J_{sc}}{J_0} + 1\right), \tag{9}$$

where the density of the saturation dark current J_0 is calculated from the equation

$$J_0 = qn_i^2 \frac{D_p}{N_d L_p} \coth\frac{d}{L_p}. \tag{10}$$

Here n_i and N_d are the intrinsic and donor carrier concentrations in the silicon substrate, respectively, and D_p is the diffusion coefficient for holes. From Eq. (10) the value of J_0 decreases with the resistivity ρ of the silicon substrate. The calculated dependence for the open-circuit voltage on the value of the resistivity of the Si substrate is shown in Fig. 7.

In order to calculate the I–V characteristics of the solar cells under illumination we need to take into account the series and shunt resistances of the cells. As a first approximation for simplifying (6) we assumed that $R_{sh} = \infty$. Then, a series resistor R_s for a square cell with a side l can be calculated as [15]

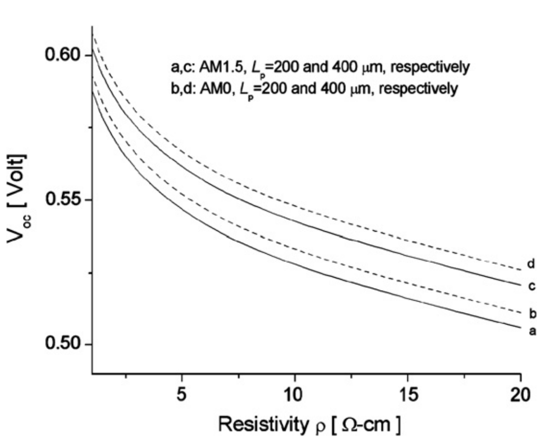

Fig. 7. Calculated dependence of the open-circuit voltage on the resistivity ρ of the Si substrate.

$$R_s = \rho_{Si}\frac{d_{Si}}{A} + \frac{b+a}{l}\left(\frac{R_s^{ITO} d_{ITO}}{8l} + \frac{R_{MC} l}{2a}\right), \tag{11}$$

where ρ_{Si}, R_s^{ITO}, R_{MC} are the resistivity of the silicon substrate, and the sheet resistances of the ITO film and the metallic contact, respectively; d_{Si} and A are the thickness and area of the silicon substrate; a is the width of a multiple strip line metallic contact, and b is the distance between neighboring contacts. The calculated series resistance for the cell with an area of 1 cm^2, $l = 1$ cm, $\rho_{Si} = 10\ \Omega$ cm, $R_s^{ITO} = 30\ \Omega/\square$, $R_{MC} = 0.017\ \Omega/\square$, $d_{Si} = 0.05$ cm, $d_{ITO} = 80$ nm, $a = 0.01$ cm, and $b = 0.25$ cm is 0.96 Ω. An additional series resistance is introduced by the thin intermediate SiO_x layer. The value of this resistance was determined by investigating the I–V characteristics of a metal–insulator–heavy doped silicon structure. These characteristics, for structures with an insulator obtained for the sample with 10 min treatment of the substrate immersed in hot H_2O_2 are ohmic, and the additional resistance was found to be 0.84 Ω. Thus, the total series resistance of the cell with an area of 1 cm^2 is 1.8 Ω. Fig. 8 shows the experimental I–V characteristics of the solar cell with an area of 1 cm^2 fabricated on 10 Ω cm silicon (dots and dashed lines) under AM0 illumination conditions. In the same figure, the calculated characteristic obtained with Eq. (6) is also shown. At the first step, this characteristic was calculated with $J_{sc} =$ 40 mA/cm^2, $R_s = 1.8\ \Omega$, and $R_{sh} = \infty$. Then, in order to obtain a best fitting with the experimental results, the calculated characteristic was corrected using $R_{sh} = 300\ \Omega$. One can see an excellent coincidence between the experimental and calculated characteristics and the parameters of the cell (fill factor F.F. and conversion efficiency η). In Fig. 8 the calculated characteristic under the AM1.5 illumination conditions is also shown. At these conditions, the value of F.F. and η are very close to the experimental parameters obtained under the AM2 illumination

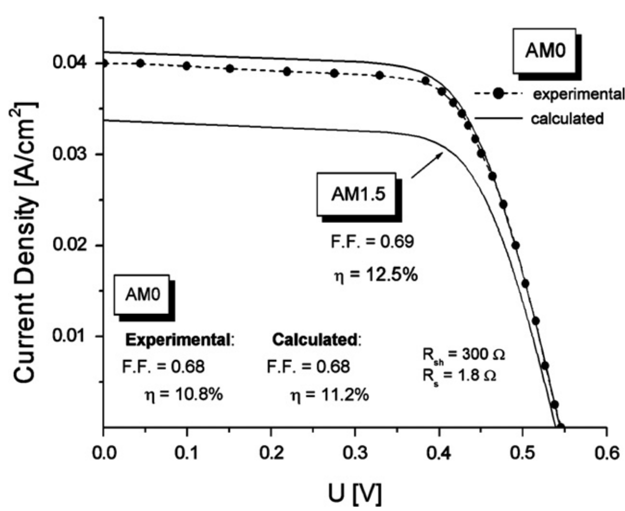

Fig. 8. Experimentally obtained I–V characteristics of the solar cell with an area of 1 cm^2 fabricated on 10 Ω cm silicon (dots and dashed line) under AM0 illuminated conditions. The calculated characteristic under AM1.5 illumination conditions is also shown.

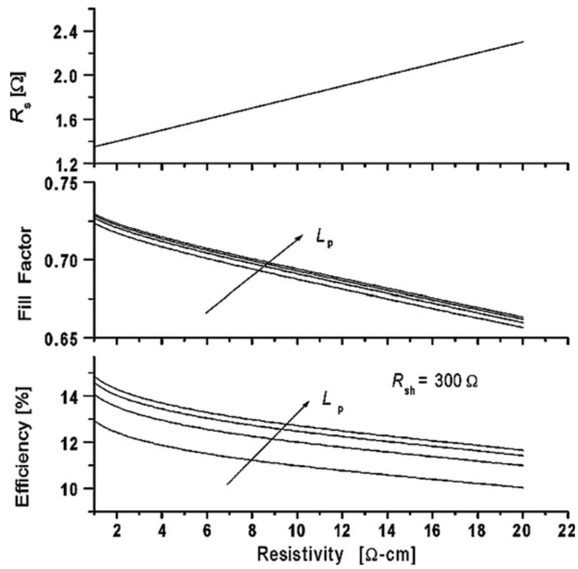

Fig. 9. Calculated parameters of the ITO–SiO_x–*n*Si solar cells for different resistivity of the silicon substrate, and under AM1.5 illumination conditions. The diffusion length increases in the direction shown by the arrow, and has values of 100, 200, 300, and 400 μm; R_s is a series resistance of the solar cell.

conditions that are 0.69% and 12.2%, respectively. The calculations show that the conversion efficiency of the ITO–SiO_x–*n*Si solar cells can be improved by using silicon with a lower resistivity. Under the AM1.5 conditions, the calculated dependences of the series resistance, fill factor, and efficiency on the resistivity of the silicon substrate are shown in Fig. 9. Solar cells fabricated on the silicon substrate with a resistivity of 1 Ω cm and a diffusion length of $L_p = 200$ μm may possess an efficiency of 14%. A further reduction of the resistivity of the silicon substrate for the experimental potential barrier at the ITO/Si interface (0.9 eV) is not possible to achieve for structures with a p–n inversion layer or minority carrier devices. Such structures are majority carrier devices, and theirs properties are described by the theory of Schottky barriers. In such cases, one can expect a lower efficiency as that reported in [5], and which was due to a higher saturation current. This is a limitation of ITO–SiO_x–*n*Si solar cells in comparison with standard p^+–n cells, in which a higher efficiency may be obtained by using the substrate with a lower resistivity (down to 0.1 Ω cm). Nevertheless, in contrast to the technique used in this work, the fabrication processes to obtain such solar cells are more laborious and expensive.

5. Conclusions

ITO–SiO_x–*n*Si solar cells have been produced using the spraying technique. The transparent and conductive tin-doped indium oxide films were made using a very simple, cheap, and fast method. The cells obtained in such a way may be considered as structures with an inversion p^+–n junction in contrast to the Schottky barrier structures reported in [5]. Under the AM0 and AM2 illumination conditions, the efficiency is 10.8% and 12.2%, respectively. Our results presented an improved efficiency in comparison to those published in [1–4], where the reported conversion efficiency was 10–11%. Our calculations based on a p^+–n model show an excellent coincidence between the theoretical and the experimental results. It was shown that using 1 Ω cm silicon substrates is a promising alternative for obtaining solar cells with a 14% efficiency under AM1.5 illumination conditions. This result is in good agreement with the theoretical calculation of the efficiency for semiconductor–insulator–semiconductor solar cells reported in [10,11]. Using substrates with a lower resistivity leads to the reduction of the conversion efficiency due to the formation of Schottky barriers presenting a higher dark saturation current than that presented by p^+–n structures.

Experimental solar modules based on this ITO–SiO_x–*n*Si cells, with an input power of 0.5–2 W, tested under the AM1.5 illumination conditions, and presenting a conversion efficiency near 11%, will be described in detail in a separate publication.

Thus, solar cells based on semiconductor–insulator–semiconductor structures are promising for solar energy conversion due to their excellent figures of merit and their relatively low cost.

References

[1] J.C. Manifacier, L. Szepessy, Appl. Phys. Lett. 31 (1979) 459.
[2] T. Feng, A.K. Ghosh, C. Fishman, J. Appl. Phys. 50 (1979) 4972.
[3] A.P. Genis, P.A. Smith, K. Singh, J.B. DuBow, Appl. Phys. Lett. 37 (1980) 77.
[4] H. Kobayashi, Y. Kogetsu, T. Ishida, Y. Nakato, J. Appl. Phys. 74 (1993) 4756.
[5] A. Simashkevith, D. Serban, L. Brus, A. Coval, V. Fedorov, E. Bobeico, Iu. Usatii, Moldavian J. Phys. Sci. 3 (2004) 334.
[6] A. Malik, A. Sêco, E. Fortunato, R. Martins, J. Non-Cryst. Solids 227–230 (1998) 1092.
[7] S. Verhaverbeke, J.W. Parker, C.F. McConnell, in: MRS Symposium Proceedings, vol. 477, 1977, p. 47.
[8] S.M. Sze, Physics of Semiconductor Devices, Wiley, NY, 1981.
[9] O. Malik, V. Grimalsky, A. Torres-J, in: Proceedings of the 16th International Conference on Microelectronics (ICM 2004), Tunisia, December 6–8, 2004, pp. 471–474.
[10] J. Shewchun, D. Burk, M. Spitzer, IEEE Trans. Electron Devices 27 (1980) 705.
[11] K.K. Ng, H.C. Card, IEEE Trans. Electron Devices 27 (1980) 716.
[12] A.L. Fahrenbruch, R.H. Bube, Fundamentals of solar cells, Photovoltaic Solar Energy Conversion, Academic, NY, 1983.
[13] O.S. Heavens, Optical Properties of Thin Solid Films, Dover, NY, 1991.
[14] <http://www.Filmetrics.com>.
[15] M. Wolf, Prog. Astronaut Rocket 3 (1961) 231.